SF2A 2006
D. Barret, F. Casoli, T. Contini, G. Lagache, A. Lecavelier, and L. Pagani (eds)

SOLID BODIES DYNAMICS IN ACCRETION DISKS: NUMERICAL SIMULATIONS AS A TOOL TO VALIDATE AN ANALYTICAL MODEL

S. Fromang[1], J. Papaloizou[1] and A. Carballido[2]

Abstract. In accretion disks, solid bodies settle toward the equatorial plane because of gas drag. However, MHD turbulence, resulting from the magnetorotational instability, significantly affects this simple picture. Indeed, small particles, initially released close to the disk equatorial plane, quickly diffuse away from the equatorial plane because they are strongly coupled to the gas. An analytical model can be used to express the diffusion coefficient as a function of the velocity correlations. Large particles, on the other hand, are weakly coupled to the gas and form a thin layer whose thickness can be expressed as the solution of a Fokker-Planck equation. In both cases, 3D MHD numerical simulations can be used as a way to confirm and support the expressions derived from these analytical models.

1 Introduction

A good understanding of dust dynamics in protoplanetary (PP) disks is crucial both for theoretical and observational reasons. On the theoretical side, dust particles are thought to be the main constituent of protoplanets. On the observational side, observations are extremely sensitive to the spatial distribution of dust grains in PP disks because of their large opacity. For both reasons, it is important to develop a reliable model that predicts the dust spatial distribution.

Because of their interaction with the gas, dust particles tend to settle toward the equatorial plane of the disk. At the same time, the gaseous turbulent motions resulting from the nonlinear evolution of the magnetorotational instability (MRI; Balbus & Hawley 1998) act as an anomalous diffusion coefficient that tends to reduce the degree of this settling. It is the purpose of this paper to study the settling processes in turbulent PP disks, by comparing analytical models with the results of numerical simulations.

2 Notations and numerical method

In PP disks, gas and dust particles are coupled through the drag force, which takes the form

$$\boldsymbol{F_D} = m_p \frac{\boldsymbol{u} - \boldsymbol{v}}{\tau_{\rm st}}\,, \tag{2.1}$$

where m_p is the mass of a dust particle, $\boldsymbol{v}$ its velocity and $\boldsymbol{u}$ is the gas velocity. In the following, we will concentrate on particles small enough to be in the Epstein regime (their size a is smaller than the gas mean free path). In that case, $\tau_{\rm st}$ takes the form (Weidenschilling 1997; Cuzzi et al. 1993)

$$\tau_{\rm st} = \frac{\rho_s}{\rho}\frac{a}{c_s}\,. \tag{2.2}$$

In this expression, ρ is the gas density, ρ_s the particles mass density and c_s the speed of sound.

In the following, we will solve the equations that described the coupled evolution of the gas and the dust. For the gas, we solve the ideal MHD equations with the code ZEUS (Stone & Norman 1992a,b), using the shearing box approximation (Hawley et al. 1995). The evolution of the dust is done as follows: if $\Omega\tau_{\rm st} \ll 1$ (Ω

[1] DAMTP, University of Cambridge, Wilberforce Road, Cambridge CB3 0WA UK
[2] Institute of Astronomy, University of Cambridge, Madingley Road, Cambridge, CB3 0HA, UK

being the angular frequency), the particles behaves as a pressureless fluid, subject only to the drag force and to gravity, and the corresponding equations are solved in a way similar to the gas. In the opposite limit, the dust particles are better described using an N–body approach (Carballido et al. 2007). In both cases, we use a box with sizes $(H, 2\pi H, 6H)$ in the radial, azimuthal and vertical directions (in the following, H stands for the disk scale height). The gas is vertically stratified and subject to the influence of a zero net flux vertical field. Our resolution throughout this paper is $(N_x, N_y, N_z) = (32, 100, 192)$.

3 Dust diffusion coefficient

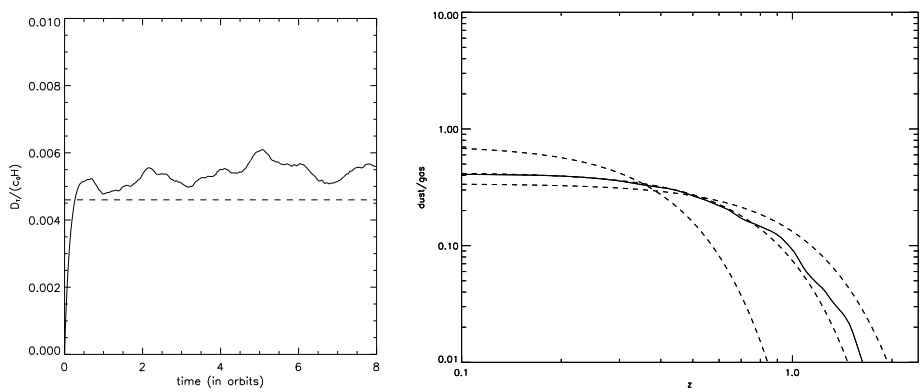

Fig. 1. The left panel shows the time evolution of the diffusion coefficient, as computed from Eq. (3.1). The dashed line represents the analytical estimates of Eq. (3.2). On the right panel, the solid line shows the vertical profile of the dust to gas ratio after 3 orbits (*solid line*). It is compared with three solutions of a simple diffusion equation obtained for three different values of the diffusion coefficient: $D_T/(c_sH) = 10^{-3}, 5.5 \times 10^{-3}$ and 10^{-2} (*dashed curves*).

Very small particles are very well coupled to the gas and essentially behave as a passive scalar. In a turbulent velocity field, they are therefore subject to a random walk as they follow turbulent eddies. In this case, it can be shown (Fromang & Papaloizou 2006) that their evolution in space should be diffusive, with an anomalous diffusion coefficient D_T that takes the form

$$D_T(\tau) = \int_0^\tau < u_z(z, \tau') u_z(z, 0) > d\tau' \,, \tag{3.1}$$

where $< . >$ denotes a suitable ensemble average. For long integration time, this expression tends toward a limit which is expected to be of the order

$$D_T \sim < u_z^2 > \tau_{corr} \,, \tag{3.2}$$

where τ_{corr} is a measure of the turbulent correlation timescale.

In order to measure the value of D_T, we performed with ZEUS a numerical simulation as described in section 2. As expected, the MRI drives MHD turbulence. The amplitude of the velocity fluctuations is in agreement with previous similar calculations (Stone et al. 1996): $\sqrt{< u_z^2 >} \sim 0.1 c_s$. We measured the time evolution of the function $D_T(\tau)$ from which τ_{corr} could be determined. The resulting curve is plotted on the left panel of Fig. 1. After a short time, it is seen to saturate at a roughly constant value: $D_T/(c_sH) \sim 5.5 \times 10^{-3}$. The analytical estimate of Eq (3.2), shown by the dashed line on Fig. 1, gives $D_T/(c_sH) = 4.7 \times 10^{-3}$. This is consistent with the numerically determined value. To check the validity of the theory, we introduce small particles in the neighborhood of the midplane of the disk. Their stopping parameter is such that $\Omega\tau_{\rm st} = 10^{-6}$. We then follow the time evolution of their spatial distribution and compare it with the solution of the standard diffusion equation. The results are summarized on the right panel of Fig. 1. The solid line shows the vertical profile of the dust to gas ratio three orbits after the dust particles are introduced. This is compared with the solution of the diffusion equation for 3 different values of the diffusion coefficient $D_T/(c_sH) = 10^{-3}, 5.5 \times 10^{-3}$ and 10^{-2}. The middle curve, which corresponds to the second case, is seen to match the simulation results quite well.

4 Settling of large particles

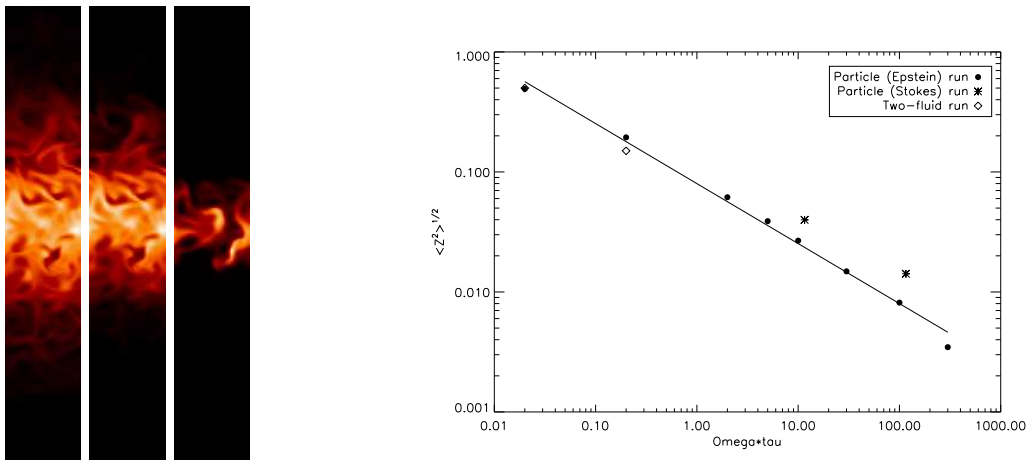

Fig. 2. Left panel: typical distribution of the dust density in the (r-z) plane of the disk for 3 different values of the coupling parameter. From left to right, they are respectively equal to $\Omega\tau_{\rm st} = 10^{-3}, 10^{-2}$ and 10^{-1}. Right panel: Dust disk scale height as a function of the coupling parameter $\Omega\tau_{\rm st}$, obtained using the two fluid description (*open circles*) and the N–body approach (*black dots*). The solid line gives the solution of the Fokker–Planck equation given by Eq. 4.2.

In the previous section, we considered only very small particles. Here, we focus on larger particles. The left panel of Fig. 2 reproduces the typical distribution of the dust particles for three different value of the coupling parameter after they reached a quasi steady state equilibrium. From left to right, the different snapshots correspond to $\Omega\tau_{\rm st} = 10^{-3}, 10^{-2}$ and 10^{-1}. Significant settling has occurred in the last case.

For larger parameter, the stopping timescale $\tau_{\rm st}$ becomes of the order of the orbital period or larger. The two fluid approach breaks down and an N–body description should be used. Using such a method, we calculated the thickness of the dust layer for values of $\Omega\tau_{\rm st}$ ranging from 10^{-2} to 300. The results are plotted on the right panel of Fig. 2 using the black dots. At the lower end of that range, they agree nicely with the results obtained with the two fluid approach, which are shown with the open circles.

These numerical results can be compared to an analytical expression for the dust disk scale height. Indeed, Carballido et al. (2007) showed that the distribution function $f(z, v_z, t)$ describing the vertical equilibrium of the particles is the solution of the following Fokker–Planck equation

$$\frac{\partial f}{\partial t} + v_z \frac{\partial f}{\partial z} + \frac{\partial}{\partial v_z}(bf) = D_{\rm v} \frac{\partial^2 f}{\partial v_z^2}, \tag{4.1}$$

where $b = -\Omega^2 z - v_z/\tau_{\rm st}$ and $D_{\rm v} = D_{\rm T}/\tau_{\rm st}^2$ is the diffusion coefficient of the particles in velocity space. The solution of this equation gives

$$H_d = \sqrt{\frac{D_T}{\tau_{\rm st}\Omega^2}}\,, \tag{4.2}$$

which is shown on the right panel of Fig. 2 by the solid line, using again $D_T/(c_s H) = 5.5 \times 10^{-3}$, according to the results of section 3. The agreement between Eq. (4.2) and the numerical results is seen to be very good, therefore validating the above analytical model.

5 Consequences for protoplanetary disks

In this section, we highlight some consequences for the global spatial distribution of dust particles in PP disks. We begin by noting that

$$\Omega\tau_{\rm st} = \Omega \frac{\rho_s}{\rho} \frac{a}{c_s} \sim \frac{\rho_s a}{\Sigma} \tag{5.1}$$

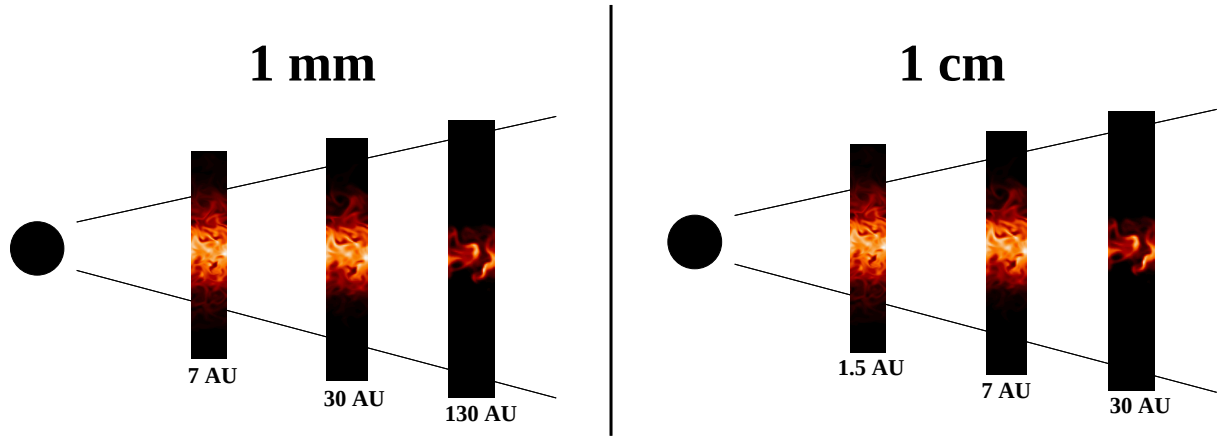

Fig. 3. Cartoon showing the dust distribution in the (r, z) plane at 3 radial locations in the disk for two different particles sizes: 1 millimeter (*left panel*) and 1 cm (*right panel*). The underlying disk model is that of the minimum mass solar nebula.

Upon choosing a specific disk model and a dust particle size, the above equation can be seen as a relation between the coupling parameter and a spatial location in the disk. For illustrative purposes, we adopt here the minimum mass solar nebula model (Hayashi et al. 1985), for which

$$\Sigma = \Sigma_0 \left(\frac{R}{1AU} \right)^{-1.5} , \tag{5.2}$$

with $\Sigma_0 = 1700 g.cm^{-2}$. Using this model, we can remap the results of the simulations presented on the left panel of Fig. 2 to a radial position in the disk. This is done in Fig. 3 for two particle sizes, 1 mm (*left panel*) and 1 cm (*right panel*). For the former, significant settling only takes places on scales of $\sim$ 100 AU or more: turbulence is very efficient at mixing these small particles, even at large distances from the central star. For centimeter size particles, for which the coupling is weaker, the dust layer is strongly settled on scales of a few tens of AU.

6 Conclusion

In this paper, we have studied the effect of MHD turbulence on the settling of dust particles of various sizes. Numerical simulations have been used as a way to validate analytical estimates for the anomalous diffusion coefficient that governs the evolution of tightly coupled dust particles and for the thickness of the layer of partially decoupled particles. We also outlined some consequences for the spatial distribution of dust particles in PP disks.

References

Balbus, S. A., Hawley, J. F. 1998, RvMP, 70, 1

Carballido, A., Fromang S., Papaloizou, J. 2007, MNRAS, submitted

Cuzzi, J.N., Dobrovolskis, A.R., Champney, J.M. 1993, Icarus, 106, 102

Fromang, S., Papaloizou, J. 2006, A&A, 452, 751

Hawley, J.F., Gammie, C.F., Balbus, S.A. 1995, ApJ, 440, 742

Hayashi, C., Nakazawa, K., Nakagawa, Y. 1985, Protostars and planets II, University of Arizona Press

Stone, J.M., Hawley, J.F., Gammie, C.F., Balbus, S.A. 1996, ApJ, 463, 656

Stone, J.M., Norman, M.L. 1992a, ApJS, 80, 753

Stone, J.M., Norman, M.L. 1992b, ApJS, 80, 791

Weidenschilling, S.J. 1977, MNRAS, 180, 57